

First-principles study of binary transition-metal clusters and alloys

This article has been downloaded from IOPscience. Please scroll down to see the full text article.

2004 J. Phys.: Condens. Matter 16 S2263

(<http://iopscience.iop.org/0953-8984/16/22/028>)

View [the table of contents for this issue](#), or go to the [journal homepage](#) for more

Download details:

IP Address: 129.252.86.83

The article was downloaded on 27/05/2010 at 15:16

Please note that [terms and conditions apply](#).

First-principles study of binary transition-metal clusters and alloys

S Dennler¹, J Morillo¹ and G M Pastor²

¹ Centre d'Elaboration de Matériaux et d'Etudes Structurales, CNRS UPR 8011, 29 rue Jeanne Marvig, 31400 Toulouse, France

² Laboratoire de Physique Quantique, CNRS UMR 5626, Université Paul Sabatier, 118 route de Narbonne, 31062 Toulouse, France

E-mail: dennler@cemes.fr

Received 30 October 2003

Published 21 May 2004

Online at stacks.iop.org/JPhysCM/16/S2263

DOI: 10.1088/0953-8984/16/22/028

Abstract

Small Co_MRh_N clusters have been studied by performing first-principles calculations in the framework of the density functional theory. In order to understand the interplay between their structural order, chemical order and magnetic properties, the corresponding bulk alloys in various hypothetically ordered phases were also calculated. In the bulk alloys and in most of the clusters there is an induced magnetic moment on the Rh atoms with increasing Co concentration which results in an increase in the average magnetic moment per atom. This effect, when present, may be twice as large in the clusters than in the corresponding macroscopic alloys. For low-symmetry clusters structures, the substitution of Rh by Co atoms results in a remarkable enhancement of the local magnetic moment at the Rh neighbours even at low Co concentration. On the other hand, the Co doping effect can be masked in cluster geometries of higher symmetry in which pure Rh clusters already show a high magnetic moment. In addition it is shown that local coordination and magnetic energy are the leading parameters for the determination of the stability and magnetic enhancement, whereas chemical order seems less important.

1. Introduction

In standard magnetic recording technology a bit of information corresponds to a small area or volume of ferromagnetic material with a well-defined mean magnetic moment (modulus M and up or down orientation along the easy axis). In order to have an appropriate signal-to-noise ratio S/N , this bit area contains a number N of magnetic particles or media grains, which conditions the density of information one can store (about 20 Gbits in^{-2} at the present time). For media limiting noise, S/N is proportional to N . In order to increase the storage capacity

one would like to reduce the size of the media grains. However, this can have two undesired effects. First, there is a reduction of the magnetic moment associated to the bit area, since M is roughly proportional to the number of atoms (i.e. to the grain volume). Unless the magnetic moments per atom are enhanced this would reduce the signal detected by the read sensor. Second, below a given size the grains tend to become superparamagnetic at room temperature, since the energy barrier between the fully degenerate up and down states is proportional to the magnetic anisotropy energy and to the grain volume³. In this case the stored information would become unstable.

However it is now well-known, both experimentally and theoretically, that the magnetic moments and magnetic anisotropy energy per atom are often enhanced in small metallic clusters as compared to the bulk crystalline state. Transition-metal particles of nanometre size, between the molecular and metallic states, are of particular interest in this context due to their intrinsically high magnetic moment, both in their atomic state and, in some cases, in the corresponding bulk material. For example, previous studies have demonstrated that small Fe_N , Co_N and Ni_N clusters exhibit magnetic moments that are significantly larger than the corresponding bulk magnetizations [1–7]. Moreover, non-vanishing magnetic moments have even been observed in small clusters of some 4d transition metals, for example Rh_N with $N \leq 50$, which are non-magnetic in the solid state.

Magnetic nanoparticle patterned media are then extensively studied as a potential breakthrough technology for high-density storage of information. As previously demonstrated, the key requirement is that the individual nanoparticles exhibit both a large magnetic moment and a high anisotropy. More generally, in the last decades, theoretical and experimental studies have shown that the reduction of size and dimensionality can give rise to a large range of novel materials with original physical and chemical behaviours. This has opened the possibility of generating specifically designed nanomaterials with tailored properties. Understanding the conditions for the development of such properties is crucial in order to be able to properly adjust and control these parameters in particular for magnetic applications.

Alloying 3d (bulk ferromagnetic) and 4d (bulk non-magnetic) elements has been found to be an effective way to induce a finite moment on the 4d atoms in the bulk state [8–10]. Due to the 3d high magnetic moments and the 4d strong spin–orbit coupling, combining this alloying effect with the size reduction effect is a promising idea to achieve both a large moment and high anisotropy. Indeed, a strong enhancement of the saturation magnetization in CoRh nanoparticles [11] compared to the bulk alloy value [8–10] was recently demonstrated, as well as a magnetic anisotropy larger than in monometallic Co particles. Therefore, besides the theoretical point of view, this motivates a systematic understanding of the microscopic properties of such 3d/4d mixed nanoparticles, for which atomic-scale calculations prove very fruitful.

In contrast to homonuclear clusters, there have been few theoretical studies on mixed transition-metal clusters, despite the steadily growing amount of experimental work and the remarkable variety of magnetic behaviours as a function of composition and chemical order. In order to achieve a better understanding of the interplay between structural, chemical and magnetic properties of these bimetallic nanoparticles, small free Co_MRh_N clusters and the corresponding bulk alloys have been studied by first-principles density functional theory calculations. Since the accurate *ab initio* simulation of such transition-element nanoparticles is particularly demanding, especially from the point of view of computational time, this study

³ The crystalline state is intrinsically anisotropic, and as a consequence the magnetic moment direction is also. The fundamental ferromagnetic state of the system corresponds to a well-defined direction (or family of equivalent directions). The magnetic anisotropy energy (MAE) is then defined as the energy difference corresponding to non-equivalent magnetization directions. The MAE controls the stability of the magnetization direction against temperature fluctuations and is therefore crucial for storage information.

has focused on Co_MRh_N with $M + N = 2-4$ and 7. In this paper our first aim is to infer general trends as a function of the structural and chemical order in the small size regime. On the one hand, this information could then be used to infer or extrapolate the behaviour of larger particles, at least from a local point of view. On the other hand, the generated database of *ab initio* results on the structure and binding energy of binary clusters, as well as the cohesive energies and surface energies of the corresponding bulk materials, can be used to define the parameters of semi-empirical approaches that are applicable to much larger particles. This would allow the theoretical exploration of the size range considered in recent experiments. Moreover, comparison between semi-empirical and *ab initio* results on the local and average magnetic moments would allow the testing of the accuracy of the latter. First of all, one would like to understand how the cluster structure, the distribution of the two species within the cluster, and the resulting magnetic moments, depend on the experimentally relevant variables like cluster size and composition. On the basis of these fundamental properties one could then focus on relativistic effects like magnetic anisotropy and orbital magnetism which are known [12–14] to depend crucially on the structure of the nanoparticles and on the characteristics of the 3d–4d interfaces within the cluster⁴.

It will be shown that in most clusters the average magnetic moment per atom is more than twice as large as that in macroscopic alloys and increases with increasing Co concentration. Co seems to retain its magnetic properties even in a highly mixed environment. For non-symmetric cluster structures, the Co doping is efficient even at low Co concentration and results in a remarkable enhancement of the local magnetic moments at the Rh neighbours larger than in the corresponding bulk alloy. On the other hand, the Co doping can be masked in cluster geometries of higher symmetry in which pure Rh clusters already show a high magnetic moment. The most stable configurations are not necessarily those of highest magnetic moment but the energy differences remain small, which implies the possibility of coexistence of several isomers. The comparison of the different bulk structures and cluster geometries shows that local coordination and magnetic energy are the key parameters that govern magnetic enhancement and stability rather than the local chemical order whose main effect is to favour mixed bonds.

The remainder of the paper is organized as follows. The theoretical framework and computational procedure are briefly described in section 2. Section 3 is devoted to the description of the limiting cases: the bulk materials and the dimers, while in section 4 the small cluster results are presented. Finally, section 5 summarizes our conclusions and points to future developments.

2. Computational details

The present calculations have been performed by means of the Vienna *ab initio* simulation program VASP developed at the Institut für Materialphysik of the Universität Wien [15]. They are based on the density functional theory (DFT) and the pseudopotential approximation, which are currently methods capable of dealing with large transition-metal clusters in a practical way. The Perdew–Wang 91 [16] generalized-gradient approximation of the exchange–correlation functional was used, which is known to give reasonably good results for transition-metal properties [17]. A detailed description of the computational parameters that have been monitored in order to control the accuracy of the results as regards the clusters calculations can be found elsewhere [17]. Concerning the bulk calculations, the only difference has been the use of a $15 \times 15 \times 15$ Monkhorst–Pack grid [18] instead of the sole Γ point to sample the first Brillouin zone.

⁴ The anisotropy energy is usually much smaller than the other relevant energy scales. This justifies dealing with its effects in a perturbative spirit, once structure and spin magnetization effects have been taken into account.

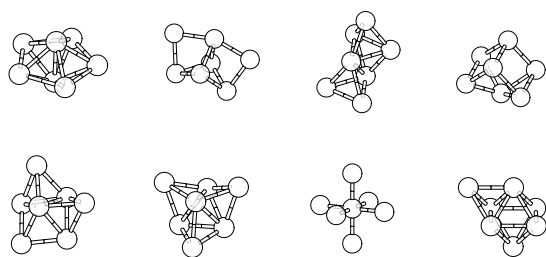


Figure 1. The different topologies that were considered as initial geometries in our exploration of the 7-atom mixed clusters.

The presence of numerous close-lying electronic configurations with different spin multiplicities or geometries makes the precise determination of the actual ground-state particularly difficult. Therefore, the geometry optimizations have been carried out for several fixed relevant values of the total spin magnetic moment S_z , and for various initial geometries in order to detect the nearby isomers. The number of possible isomers increases very rapidly with increasing cluster size: therefore, while it was computationally feasible to consider all possible geometries for the smallest 3- and 4-atom clusters, our investigation had to focus on some particular geometries in the case of the 7-atom series. These selected geometries are illustrated in figure 1. Reported local magnetizations $\mu(i)$ have been obtained by integration of the magnetization density in spheres centred on each atom with radii $r_{\text{sph}}(\text{Co}) = 1.30 \text{ \AA}$ and $r_{\text{sph}}(\text{Rh}) = 1.40 \text{ \AA}$.

3. Bulk alloys and dimers

3.1. Bulk alloys

Results for the Co and Rh periodic solids and for $\text{Co}_x\text{Rh}_{1-x}$ bulk alloys are summarized in figure 2. Co and Rh possess the same spin moment in their atomic state ($3 \mu_{\text{B}}$ /atom in the d^7s^2 and d^8s^1 configurations, respectively) but exhibit completely different behaviours as bulk crystals.

For bulk Co the stability of the hexagonal close packed (hcp) structure is correctly reproduced by the DF calculations. The optimized lattice parameters $a = 2.493 \text{ \AA}$ and $c = 4.023 \text{ \AA}$ compare very well with experimental results ($a^{\text{exp}} = 2.507 \text{ \AA}$ and $c^{\text{exp}} = 4.069 \text{ \AA}$). The same holds for the spin magnetic moment per atom $\mu_{\text{b}}(\text{Co}) = 1.58 \mu_{\text{B}}$ ($\mu_{\text{b}}^{\text{exp}}(\text{Co}) = 1.57 \mu_{\text{B}}$). The comparison of magnetic and non-magnetic calculations (figure 2(b)) reveals the large contribution of magnetism to the cohesion which, in the case of Co, turns out to be at the origin of the stabilization of the hcp phase in agreement with previous local spin density calculations [19]. Notice that the magnetic contribution (170–208 meV/atom) is large compared to the energy difference between the hcp and the fcc phases ($\sim 18 \text{ meV/atom}$). In the case of Rh, the face-centred cubic (fcc) structure is more stable than the hcp one with lattice parameter $a = 3.843 \text{ \AA}$ ($a^{\text{exp}} = 3.804 \text{ \AA}$) and vanishing magnetization.

Experimentally, the Co–Rh bulk alloys are known to form a continuous series of disordered solid solutions [20]. At room temperature their structure is fcc for a Co concentration $x_{\text{Co}} \leq 49.5\%$ and hcp for higher concentrations. Different bulk ordered alloy structures ($L1_0$, $L1_2$, and DO_{22}) based on the fcc structure with different compositions have been considered as well as one bcc-based structure (B2). The cohesive energies of the different fcc phases are nearly the same for a given composition showing an almost linear dependence with Co concentration in the non-magnetic calculations. This is a clear indication that in the absence of magnetism the alloy behaves like an ideal fcc-based solid solution where local chemical order is not important as far as the coordination does not change. Indeed, a sensible energy difference

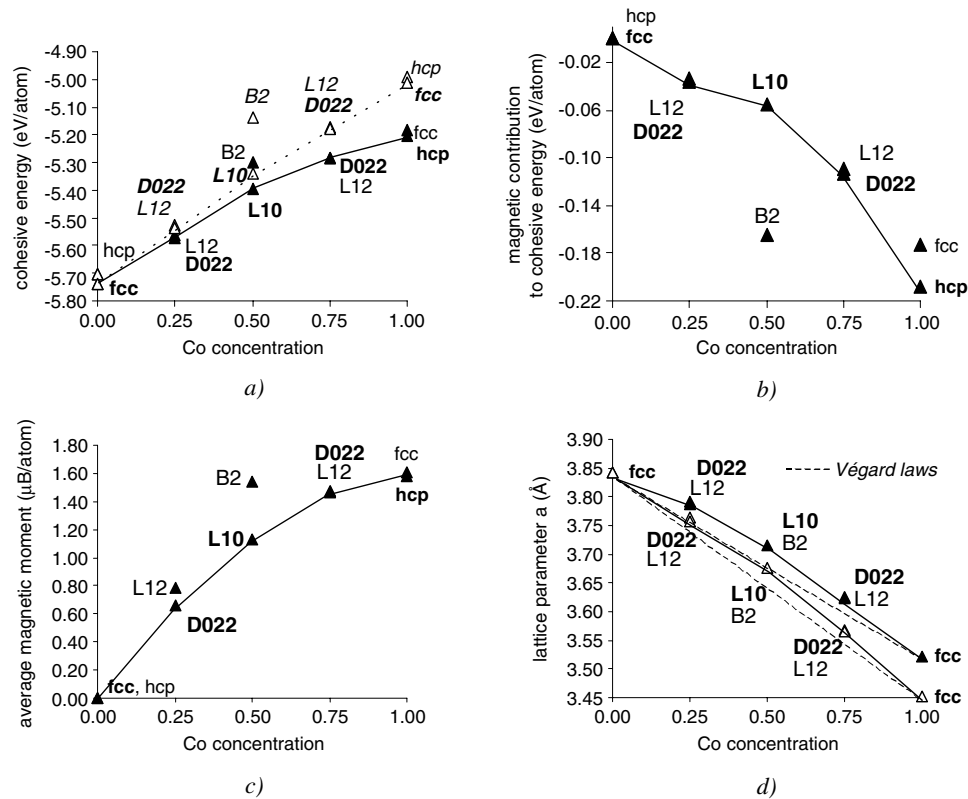


Figure 2. Structural and magnetic properties of macroscopic $\text{Co}_x\text{Rh}_{1-x}$ alloys, as a function of the Co concentration: (a) cohesive energy E_c for magnetic (▲) and non-magnetic (△) calculations, (b) magnetic contribution to E_c , (c) average magnetic moment per atom, and (d) equilibrium lattice constant a for the cubic structure, for magnetic (▲) and non-magnetic (△) calculations. The lines are a guide to the eye.

appears only between the fcc ($L1_0$) and the bcc (B2) phases at the equiatomic composition. Magnetism, when taken into account, has an increasing non-linear stabilization effect with increasing Co concentration, which induces a deviation from the previous ideal solution and a lattice parameter expansion that amounts to about 2% for pure Co.

As shown in figure 2, the average magnetic moment also increases in a non-linear way with increasing x_{Co} . This non-linear behaviour is the result of an increasing induced magnetic moment on the Rh atoms with increasing x_{Co} , marginally compensated by a very slight decrease of the Co one. Despite the fact that our calculations refer to ordered fcc-based structures, the obtained local magnetic moments are in better agreement with the experimental ones [8] than previous TB-LMTO-ASA calculations [9] in the case of Co_3Rh .

From the structural point of view, the decreasing Vegard law for the optimized lattice parameter a is approximately reproduced. The slight discrepancy seems to be due to the fact that the calculated structures are ordered ones. Calculations on disordered structures are currently in progress to clarify this point.

In summary, concerning the bulk state one may conclude that the local coordination and magnetic energy are much more important than the local chemical order, and that increasing Co concentration results in an increasingly strong magnetic energy contribution associated to an induced Rh magnetic moment and an interatomic distance contraction.

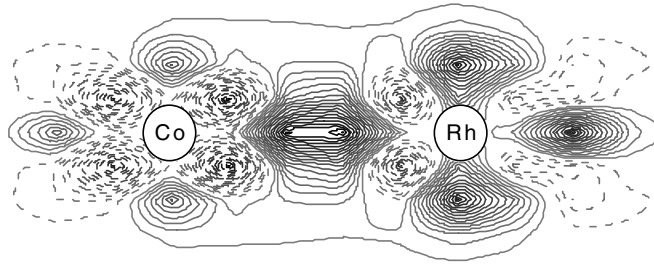


Figure 3. Contour plot of the electronic density transfer $\Delta\rho$ occurring during the formation of the Co–Rh dimer from the isolated atoms. Isolines are shown for $\Delta\rho = -0.38$ to $0.38 e \text{ \AA}^{-3}$ with an interval of $\Delta\rho = 0.02 e \text{ \AA}^{-3}$. Plain (dotted) isolines correspond to positive (negative) $\Delta\rho$.

Table 1. Cohesive energy E_c (eV/atom), total magnetic moment S_z (μ_B), integrated local magnetic moments $\mu(M)$ (μ_B), and equilibrium bond length d (\AA) of the dimers.

	Rh–Rh	Co–Rh	Co–Co
E_c	–1.71	–1.83	–1.53
S_z	4	4	4
$\mu(\text{Co})$		2.29	1.93
$\mu(\text{Rh})$	1.82	1.43	
d	2.21	2.08	1.96

3.2. Dimers

Results for the dimers are given in table 1. As usual in small clusters, the interatomic distances d are strongly reduced ($\approx 20\%$) with respect to the corresponding solids due to the lower coordination but the observed trends are the same as in the bulk materials ($d_{\text{Co–Co}} < d_{\text{Co–Rh}} < d_{\text{Rh–Rh}}$).

The mixed dimer is found slightly more stable than the pure ones. This can be easily explained by the energy difference between the highest occupied Kohn–Sham eigenvalues of the isolated atoms ($E_{\text{HOMO}}(\text{Co}) - E_{\text{HOMO}}(\text{Rh}) = 0.88 \text{ eV}$) or by their empirical Pauling electronegativities ($\chi_P(\text{Co}) = 1.88$ and $\chi_P(\text{Rh}) = 2.28$), both effects being favourable to a Co to Rh electron transfer (this is illustrated in figure 3). As a consequence there is a marked preference for mixed bonds at the expense of pure ones, a result that in principle should favour the appearance of bulk ordered structures. However, this is not the case since the solid state alloys form a quasi ideal disordered solid solution. One can then conclude that the corresponding energy gain, $E_c(\text{CoRh}) - 1/2(E_c(\text{CoCo}) + E_c(\text{RhRh})) = -0.21 \text{ eV}$, progressively disappears when approaching the bulk state due to the higher coordination. Thus, the effect might be significant only in the smallest clusters or at the cluster surface.

The average spin magnetic moment $\bar{\mu} = 2 \mu_B/\text{atom}$ is reduced compared to the isolated atoms ($\mu_{\text{at}} = 3 \mu_B$), but is significantly larger than for the macroscopic bulk alloys. This holds in spite of the shorter interatomic distance whose decreasing effect is overcompensated by the much lower coordination enhancement effect. Remarkably $\bar{\mu}$ is found to be independent of the composition, but at the local level the Co moment is slightly enhanced to the detriment of the Rh one. This can also be qualitatively explained by the previously quoted charge transfer from the 3d Co orbitals to the 4d Rh ones, which results in a polarization of a larger number of d holes on the Co atom and a corresponding reduction on the Rh one.

In conclusion, there is a larger tendency to form heteroatomic bonds at the dimer level compared to the bulk state. Moreover, the low coordination overcomes the short interatomic

distance effect resulting in a larger magnetic moment, which appears to be independent of the composition. This may favour a high magnetic moment in the clusters coupled to a high magnetic anisotropy in the alloying process. However, in contrast to what happens in the bulk alloy state, there is a tendency to a magnetic moment enhancement on the Co atom at the expense of the Rh one. One must then expect a transition from one behaviour to the other with increasing cluster size. Consequently, the correlation between Co doping and magnetic Rh enhancement need not be simple.

4. Small Co_MRh_N clusters

Cohesive energies and magnetic moments per atom for the most stable clusters with $M + N = 3$ and 4, as well as those of the ground state for $M + N = 7$ are reported in figure 4. As expected from the dimer and bulk results the increased coordination of the clusters relative to the dimer removes in most cases the stabilizing effect of mixed bonds. In fact, there is a regular decrease of the cohesive energy with increasing x_{Co} like in the macroscopic limit for any given geometry. Even if in some specific cases, at low Co concentration, when there is a maximum number of mixed bonds at the sites with lowest coordination, one can observe either a slight stabilization of a mixed isomer (e.g., Co_2Rh_5 and linear Co_1Rh_2) or a tendency to stabilization (e.g., triangular Co_1Rh_2). Nevertheless, if one compares different isomers with the same composition there remains, in general, a slight tendency to form heteroatomic bonds, as for example in the case of the two Co_2Rh_2 planar structures separated by a small 40 meV/atom energy difference. As a consequence, in Rh rich clusters the Co impurities avoid being first neighbours.

From the geometrical point of view, due to the larger coordination, the interatomic distance contraction relative to the bulk is less pronounced than in the dimer. Bond lengths are in general shorter for the less coordinated structures and the interatomic distances increase with cluster size. The significant contribution of magnetism to the geometry can be seen in the observed much larger ($\approx 5\%$) dilation of the interatomic distance in the magnetic structures with respect to the non-magnetic ones. This effect is stronger in the clusters than in the bulk alloy ($\approx 2\%$ for pure Co). As usual the most stable clusters for a given composition are the most compact ones: triangular structures for $M + N = 3$, tetrahedrons for $M + N = 4$, decahedrons (pentagonal bipyramids) and capped square bipyramids for $M + N = 7$. Here, as in the bulk, there is a significant contribution of magnetism to the stability: the magnetic structures are more stable than the non-magnetic ones, an effect that increases with increasing x_{Co} .

All mixed clusters are found to be magnetic with an average magnetic moment per atom $\bar{\mu}$ that is smaller than for the isolated atoms but remarkably enhanced with respect to the macroscopic bulk alloys. For a given cluster size, $\bar{\mu}$ increases with increasing x_{Co} . Notice that the most stable isomers are not usually the most magnetic ones as one can see for example in figure 4 for some structures. However, the energy differences always remain small, which implies the possible coexistence of several isomers.

As previously pointed out, even if the average magnetic moment globally increases with increasing x_{Co} , there is no simple correlation between Co substitution and enhancement of the Rh magnetic moments. In the considered size range, Rh_N clusters are in general magnetic and their magnetic properties are intrinsically linked to their geometry. For low-symmetric open structures, like for example the linear Rh_3 and some Rh_7 isomers, or singular non-magnetic clusters like the tetrahedral Rh_4 , the Co substitution has an efficient spin-polarization effect, even at low Co concentration, and results in a remarkable increase of the local magnetic moments at the Rh neighbours. In this case, the magnetic enhancement can reach more than $1 \mu_{\text{B}}/\text{Rh}$ atom. On the other hand, the effect of Co doping can be masked in geometries of higher symmetry in which pure Rh clusters already show a high magnetic moment. This

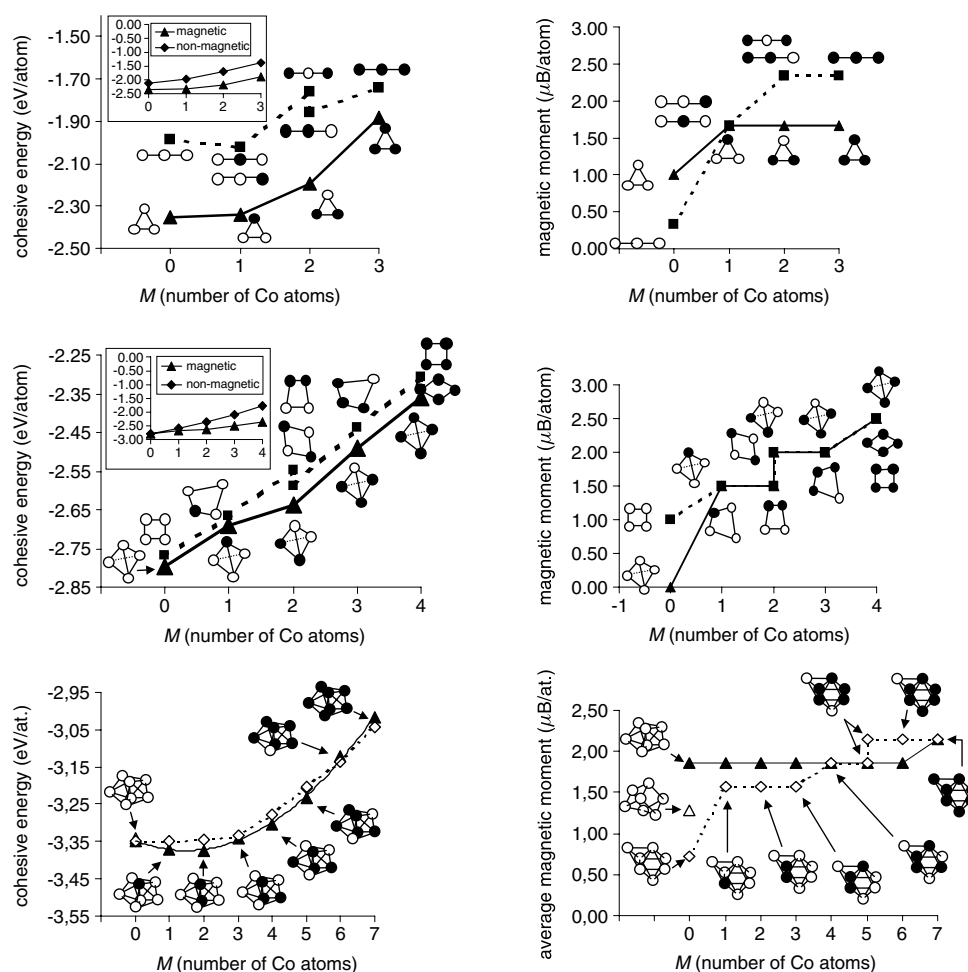


Figure 4. Cohesive energy and average magnetic moment of small Co_MRh_N clusters with $M + N = 3, 4$ and 7 as a function of the Co concentration. Results are given for the ground state configurations as well for the first excited isomers. For the sake of clarity, the structures of the 7-atom isomers are only drawn once (left: decahedral series, right: capped bipyramid series). The insets show results for magnetic (\blacktriangle) and non-magnetic (\blacklozenge) calculations. The lines are a guide to the eye.

is the case for example for the most stable 7-atom decahedral structure in which the pure Rh cluster exhibits a very large magnetic moment of $13 \mu_B$. For this size and geometry, Co doping turns out to have a weak polarization effect, since almost all mixed clusters stabilize the same moment as the pure Rh one. This leads to a plateau in the S_z versus x_{Co} curve. From the Co point of view, one observes that the Co atoms retain their magnetic moments even in a Rh-rich environment. In some cases, a small enhancement of the local Co moments is found similar to that in the CoRh dimer.

In order to better understand the origin of the Co-induced Rh magnetic enhancement, detailed calculations on constrained geometries have been performed. For example, in the case of the linear trimer presented in figure 5, the substitution of one Rh by Co in Rh_3 results in an increased Rh–Rh distance between the two remaining Rh atoms, an effect which is known to favour magnetism. In order to uncorrelate the effects of the substitution itself and those

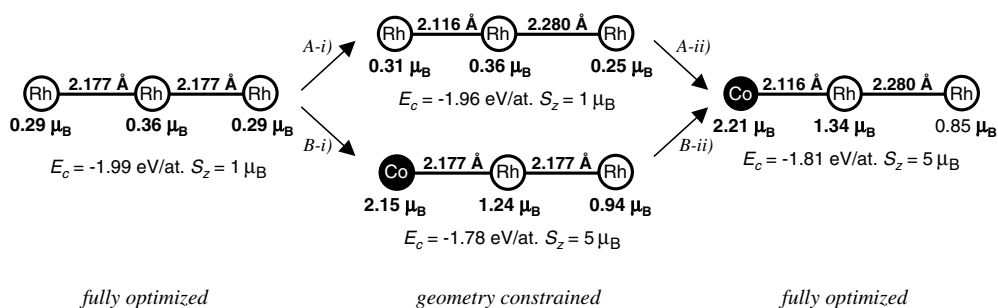


Figure 5. Local distribution of magnetic moments and nearest-neighbour bond lengths for fully optimized and geometry constrained linear Rh_3 and CoRh_2 clusters.

resulting from the induced distance variation, the doping process has been decomposed in two steps in two different manners: a geometrical deformation of the pure Rh_3 cluster, then the replacement of one extremal Rh atom by a Co one in the previous geometry (way A); or the substitution at fixed geometry applied to the pure Rh_3 , followed by a geometrical deformation of the obtained CoRh_2 cluster (way B). One observes on figure 5 that the main contribution to the magnetic enhancement at Rh atoms results from the Co substitution rather than from the sole distance variation at fixed composition. It should be also noted, however, that distance dependent effects may also play a significant role in some cases. For example, a bond-length expansion of less than 5% yields an increase of 2 μ_B in the total moment of Rh_3 .

5. Conclusion

These calculations have shown that small CoRh clusters are magnetic with average moments that are significantly larger than those of the corresponding bulk materials and increase with Co concentration. Moreover, Co seems to retain its magnetic properties even in a highly mixed environment. However as inferred from the bulk and dimer results, there is no simple correlation between Co substitution and the existence of an induced Rh magnetic enhancement. For weakly magnetic Rh_N structures, the Co doping is an efficient means of increasing the spin polarization even at low Co concentration. This results in a remarkable enhancement of the local magnetic moments at the Rh neighbours. On the other hand, the effect of Co doping can be masked in geometries of higher symmetry in which pure Rh_N clusters already show a high magnetic moment.

From the structural point of view, there is in the clusters a stronger tendency to form mixed bonds than in the bulk alloys and the energy differences between the different isomers remain relatively small, which implies the possible coexistence of several isomers in the experimental preparations. This stresses again the interest of determining not only the ground-state structures but also the first low-lying isomers, particularly since the experimental synthesis conditions and matrix effects could lead preferentially to constrained structures.

The mean magnetic moment per atom extrapolated to the equiatomic composition decreases with the cluster size, a result in qualitative agreement with those experimentally observed for nanometre-size particles [11]. Since it turns out that a few Co impurities are sufficient to get a significant magnetic enhancement, one can infer that mixed nanoparticles with a low Co concentration could be particularly attractive, showing both a large magnetic moment due to the alloying effect as well as an enhanced anisotropy due to the high Rh content.

Our results should be complemented by further investigations, since it is still unclear to what extent the observed trends are specific to the very small sizes considered here. DFT

and semi-empirical calculations of larger clusters, of low-index Rh (Co) surfaces with in- or sub-surface Co (Rh) impurities modelling the surface of much larger nanoparticles, should allow us to get a finer insight into the possible segregation and surface contribution to the magnetic properties. Finally, starting from these optimized structures, it would be worthwhile performing calculations including spin-orbit coupling and non-collinear magnetism in order to quantify to what extent the presence of the rhodium atoms induces a significant magnetic anisotropy in these clusters.

Acknowledgments

Helpful discussions with M Respaud, D Zitoun, M J Casanove and M C Fromen are gratefully acknowledged. This work has been financed in part by the EU GROWTH project AMMARE (G5RD-CT-2001-00478). Computer resources were provided by CALMIP and IDRIS (France). The calculations have been performed using the VASP *ab initio* total-energy and molecular-dynamics program (Vienna *ab initio* simulation program) developed at the Institut für Materialphysik of the Universität Wien.

References

- [1] Billas I M L *et al* 1994 *Science* **265** 1682
- Apsel S E *et al* 1996 *Phys. Rev. Lett.* **76** 1441
- [2] Respaud M *et al* 1999 *Phys. Rev. B* **59** R3934
- [3] Lee K *et al* 1985 *Phys. Rev. B* **30** 1724
- Lee K *et al* 1985 *Phys. Rev. B* **31** 1796
- Pastor G M *et al* 1989 *Phys. Rev. B* **40** 7642
- [4] Jamorski C *et al* 1997 *Phys. Rev. B* **55** 16
- Pereiro M *et al* 2001 *Int. J. Quantum Chem. A* **81** 422–30
- [5] Jinlong Y *et al* 1994 *Phys. Rev. B* **50** 11
- Chien C H *et al* 1998 *Phys. Rev. A* **58** 3
- [6] Castro M *et al* 1997 *Chem. Phys. Lett.* **271** 133
- Reddy B V *et al* 1998 *J. Phys. Chem. A* **102** 1748
- Reuse F A and Khanna S 1999 *Eur. Phys. J. D* **6** 77
- [7] Pastor G M 2001 *Atomic Clusters and Nanoparticles (NATO ASI Series, Les Houches Session LXXIII)* ed C Guet, P Hobza, F Spiegelman and F David (Berlin: Springer) p 335
- [8] Harp G R *et al* 1994 *J. Appl. Phys.* **76** 6471
- Harp G R *et al* 1995 *Phys. Rev. B* **51** 12037
- [9] Moraitis G *et al* 1996 *Phys. Rev. B* **54** 7140
- [10] Dennler S *et al* 2004 at press
- [11] Zitoun D *et al* 2002 *Phys. Rev. Lett.* **89** 037203
- Fromen M C *et al* 2002 *J. Magn. Magn. Mater.* **242–246** 610
- [12] Pastor G M *et al* 1995 *Phys. Rev. Lett.* **75** 326
- [13] Guirado-López R *et al* 2003 *Phys. Rev. Lett.* **90** 226402
- [14] Guirado-López R *et al* 2003 *Eur. Phys. J. D* **24** 73
- Muñoz-Navia M *et al* unpublished
- [15] Kresse G and Hafner J 1993 *Phys. Rev. B* **47** 558
- Kresse G and Furthmüller J 1996 *Phys. Rev. B* **54** 11169
- [16] Ziesche P and Eschrig H (ed) 1991 *Electronic Structure of Solids '91* (Berlin: Akademie Verlag)
- Perdew J P *et al* 1992 *Phys. Rev. B* **46** 6671
- [17] Dennler S *et al* 2003 *Surf. Sci.* **532–535** 334–40
- Dennler S *et al* 2003 *Eur. Phys. J. D* **24** 237–40
- [18] Monkhorst H J and Pack J D 1976 *Phys. Rev. B* **13** 5188
- [19] Min B I *et al* 1986 *Phys. Rev. B* **33** 7852
- [20] Koster W and Horn E 1952 *Z. Metallk.* **43** 444